Articles

A New Hydroxyapatite/Glass Biphasic Material: In Vitro Bioactivity

A. Rámila, S. Padilla, B. Muñoz, and M. Vallet-Regí*

Departamento de Química Inorgánica y Bioinorgánica, Facultad de Farmacia, UCM E-28040, Madrid, Spain

Received July 4, 2001. Revised Manuscript Received March 18, 2002

A new biphasic material composed of hydroxyapatite and a bioactive glass has been synthesized. The starting materials were hydroxyapatite (HA), synthesized by a wet method, and gel obtained by a sol−gel method with composition in mol %, $55SiO_2-41CaO-4P_2O_5$ (55S), both prepared before the mixture. This mixture was performed mechanically and had a final ratio HA/55S glass of 80:20. In vitro assays of bioactivity were carried out to compare the behavior of the three materials. The biphasic material has shown good bioactivity, establishing that the addition of the bioactive glass to the hydroxyapatite accelerates the formation of a hydroxyapatite layer, enhancing the bioactivity of the synthetic HA.

Introduction

Implantable materials need to have the ability of being bioactive, which means that they should be able to promote bone-tissue formation at their surface and bond to osseous tissues when implanted. In this sense, different ceramic materials have been studied as candidates.[1] Such ceramics should be able to bond to living tissues by the generation of a layer rich in calcium phosphates, which exhibit an apatite-like structure. Implants made of bioactive materials react chemically with body fluids in a manner compatible with the repair processes of the tissues. Thus, the formation of a fibrous capsule is prevented by the adhesion of the repairing tissues and the failure possibilities of the implant decrease.

Taking into account that hydroxyapatite (HA, $Ca_{10}(PO_4)_6(OH)_2$) is very close chemically to biological apatite present in human bones, it seems an adequate material to be used for these applications.[2,3] However, it presents the disadvantage of exhibiting slow bioactivity in simulated body fluid (SBF). Some references mention the slow rate of HA bioactivity;[4,5] in fact, in vitro experiments in our group have shown no signs of bioactivity after 8 weeks of assay even when the HA studied had low crystallinity. Hence, considering the chemical similarity of synthetic hydroxyapatite to the inorganic component of bone and its osseoconductive properties in vivo,[6,7] it seems interesting to find some othermaterial that could be added to HA to accelerate its bioactivity.

In this sense, glasses belonging to the $SiO_2-CaO-P_2O_5$ system obtained by the sol−gel method have proved to be highly bioactive,[8−12] and in particular the glass with composition in mol %, $55SiO_2-41CaO-4P_2O_5$ (55S),[9] shows a high growth kinetics of carbonate hydroxyapatite layer, inherent to these kind of bioactive materials.

Therefore, the aim of this work is to obtain a biphasic material (BPM) in which the main component is HA, which emulates the bone mineral component, and the glass provides the highly bioactive component. The objective is to apply glass bioactivity to accelerate the synthetic HA reactivity response toward the formation of biological apatite.

With this purpose, the in vitro bioactivity of a new biphasic material constituted by 80% HA and 20% 55S glass will be assessed. In addition, results will be compared with those obtained for both starting materials in the same conditions.

Experimental Section

55S was obtained as explained previously[9] and the synthesis of HA was carried out as follows. An aqueous slurry of $Ca(OH)_2$

* To whom correspondence should be addressed. Tel.: 34913941861. Fax: 34913941786. E-mail.vallet@farm.ucm.es.

(1) Vallet-Regí, M. *J. Chem. Soc., Dalton Trans.* **2001**, 97.
(2) Suchanek, W.; Yoshimura, M. *J. Mater. Res.* **1998**, *12*, 94.
(3) Heise, U.; Osborn, J. F.; Duwe, F. *Int-Orthop.* **1990**, *14*, 329.
(4) Nakamura, T.; Neo, M.; Kokubo, T. *Mineralization in Natural and Synthetic Biomaterials*; Li, P., Calvert, P., Kokubo, T., Levy, R., Scheid, C., Eds.; Materials Research Society: Boston, 1999; p 15.
(5) Hench, L. L.; Wilson, J. *An Introduction to Bioceramics*; Hench, L. L., Wilson, J., Eds.; World Scientific: Singapore, 1993; pp 1−24.
(6) Maxian, S. H.; Zawaddsky, J. P.; Dunn, M. G. *J. Biomed. Mater. Res.* **1994**, *28*, 1311.
(7) Moroni, A.; Caja, V. L.; Egger, E. L.; Trinchese, L.; Chao, E. Y. S. *Biomaterials* **1994**, *15*, 926.
(8) Vallet-Regí, M.; Romero, A. M.; Ragel, V.; Legeros, R. Z. *J. Biomed. Mater. Res.* **1999**, *44*, 416.
(9) Vallet-Regí, M.; Izquierdo-Barba, I.; Salinas, A. J. *J. Biomed. Mater. Res.* **1999**, *46*, 560.
(10) Pérez Pariente, J.; Balas, F.; Vallet-Regí, M. *Chem. Mater.* **2000**, *12*, 750.
(11) Vallet-Regí, M.; Rámila, A. *Chem. Mater.* **2000**, *12*, 961.
(12) Vallet-Regí, M.; Arcos, D.; Pérez-Pariente, J. *J. Biomed. Mater. Res.* **2000**, *51*, 23.

10.1021/cm011165p CCC: $22.00
Published on Web 05/03/2002

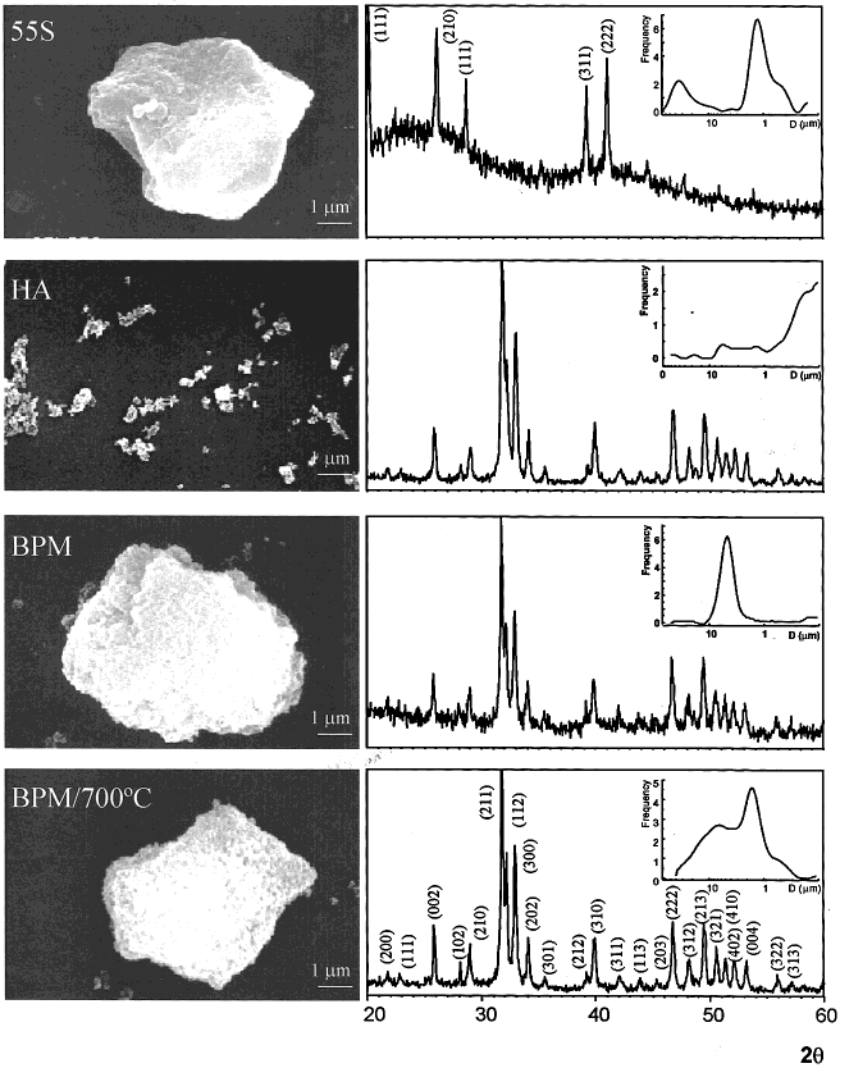

Figure 1. SEM micrographs of 55S, HA, BPM, and heated BPM are shown. Also particle size distributions and XRD patterns of the materials are displayed.

(Riedel-DeHäen) was neutralized with H_3PO_4 (Merck) solution by adding it to the $Ca(OH)_2$ suspension until the pH reached 7.1 and the mixture was stirred for 30 min at 90 °C. The HA slurry was aged for 24 h at room temperature, decanted, and vacuum-filtered. The cake was dried at 105 °C for 12 h and triturated in mortar.

The product obtained was characterized by XRD using a Philips X'Pert MPD diffractometer and the particle size distribution was determined by sedimentation using a Sedigraph Micromeritics 5100 size analyzer.

The mixture was prepared from the hydroxyapatite dried at 105 °C and the gel was dried before it was sintered so that a homogeneous mixture can be obtained. To calculate the amount of gel that will lead to the theoretical 20% of glass, thermogravimetric and differential thermal analyses of the dried gel were carried out using a Seiko Thermobalance TG/DTA 320. HA and gel were grounded for 24 h, and fractions of 0.5 g of powder were compacted at 50-MPa uniaxial pressure and 150 MPa of isostatic pressure to obtain disks (13 mm in diameter and 2 mm in height). The as-obtained disks were sintered at 700 °C for 3 h.

The assessment of the in vitro bioactivity of both HA and BPM was carried out with the same procedure that is utilized for 55S glass.[9] Samples were immersed in simulated body fluid (SBF), and changes in solution composition and pH were measured after different times of soaking on an Ilyte $Na^+K^+Ca^{2+}$pH system.

The newly formed layer was characterized by scanning electron microscopy and energy-dispersive spectroscopy (SEM-ESD) in a JEOL 6400 microscope at 20 kV and by XRD in a Philips X'Pert MDP diffractometer.

Changes in porosity were monitored by Hg intrusion on a Micromeritics Autopore III 9420.

Results and Discussion

Characterization of Materials. Figure 1 shows particle distribution and morphology of the HA, the 55S dried gel, and the BPM (both before and after heating at 700 °C), together with their respective XRD patterns. Both morphology and size of particle of 55S and HA are very different. 55S exhibits a bimodal distribution centered at 30.16 and 1.13 μm, although the micrograph shows only one size of particle to compare the morphologies of each material. On the other hand, 50% of the particles of HA have an equivalent diameter smaller than 0.13 μm. The synthesized mixture has a homogeneous distribution with a size of 7.88 μm, and its micrograph suggests that BPM is constituted by 55S particles covered by HA. This morphology does not significantly change after heating the mixture at 700 °C, although particle size distribution is bimodal with maxima centered at 10.59 and 1.94 μm.

The XRD pattern of the dried gel shows the amorphous band and the maxima corresponding to calcium

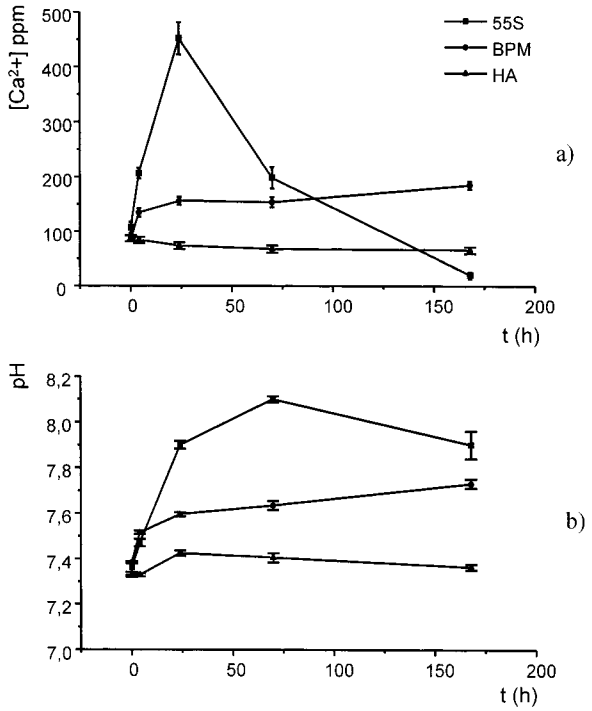

Figure 2. Changes in both [Ca^{2+}] and pH of SBF are shown for 55S, BPM, and HA.

nitrate, still present in the material before heating, and only one phase (ASTM-9−432) is present in the synthesized HA. The pattern of the biphasic mixture shows the maxima of HA with a noisy background, which can be attributed to the glassy component. When the mixture is sintered at 700 °C, the (112) diffraction maximum is better defined, the background decreases, and all the peaks are sharper, indicating a higher crystallinity.

Chemical Reactions. Figure 2 shows variations in Ca^{2+} concentration and pH for the in vitro assays of HA, 55S, and BPM. While the calcium concentration remains nearly constant during the assay for HA, changes are observed when 55S and BPM were soaked in SBF. Ca^{2+} concentration rapidly increases for 55S because of its high Ca initial content and solubility, while this increase is smoother and more continuous for BPM. After 24 h of immersion in the solution, in the case of 55S, the Ca^{2+} concentration has reached its maximum value and starts decreasing.

In Figure 2b it can be observed how the pH for the HA assay does not significantly change, whereas it increases for both 55S and BPM. In agreement with the Ca^{2+} variations mentioned above, the increase of pH is stronger for the glass, although in both cases the pH augmentation occurs mainly during the first day of the assay, and then the changes are milder.

Formation of the Apatite-like Layer. Because no significant changes are observed for HA, only bulk and glancing-angle incidence XRD patterns of the biphasic material before and after soaking in SBF are shown in Figure 3. Because the newly formed layer consists of an apatite-like phase, similar to the HA component of the starting material, no significant changes along the time frame are expected for the bulk XRD. However, in the glancing-angle incidence XRD, the initial pattern of BPM, in which (002), (210), (211), (112), (300), and

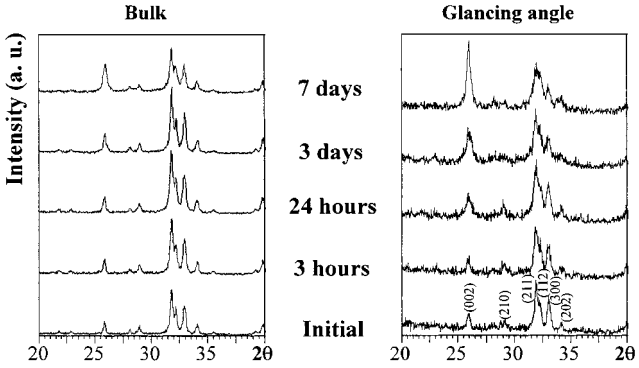

Figure 3. XRD pattern of BPM before and after soaking in SBF are shown at both bulk and glancing-angle incidences.

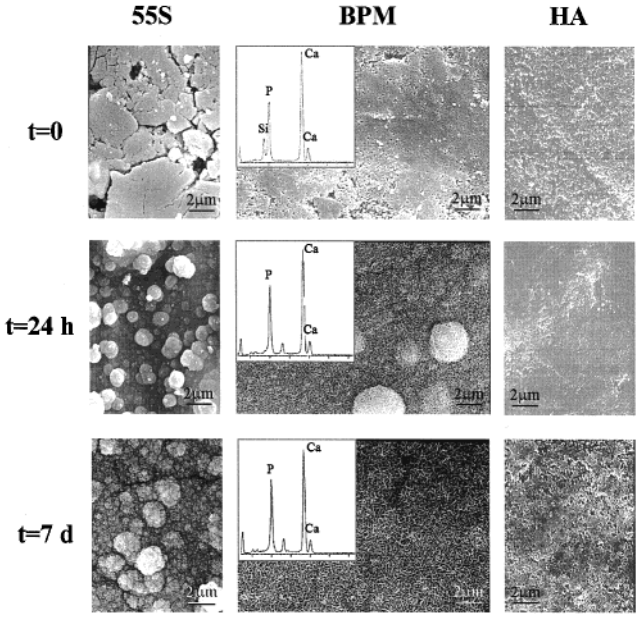

Figure 4. SEM micrographs of 55S, BPM, and HA are shown before and after soaking in SBF, together with their corresponding EDS patterns.

(202) reflections of the apatite are distinguishable, starts showing a widening of these maxima after being soaked in SBF. Besides, the relative intensity of (002) reflection increases as a function of soaking time, and after a week of assay (002) is even more intense than (211). These observations suggest the formation of an apatite-like phase, less crystalline than the HA present in the BPM, and with a preferred orientation on the crystals growth.

SEM micrographs of HA, 55S, and BPM before and after different times of soaking in SBF are shown in Figure 4. Original materials present several textural differences. While 55S shows a heterogeneous surface, BPM is similar to HA, with a more homogeneous surface. When these materials are soaked in SBF, HA shows no modifications, whereas 55S and BPM start to become covered by a new material. However, this covering is different for these two materials. After 24 h of immersion in SBF 55S is covered by a layer of spherical particles of 1−2 μm in diameter while in the case of BPM these spheres are bigger (up to 5 μm in diameter) and are constituted by hundreds of needle-like aggregates that completely cover the surface. These kind of aggregates do not appear for 55S until 7 days of soaking in SBF and even then the needle-like ag-

gregates are somehow smaller. After this period of time the spherical particles of BPM cannot be distinguishable and only the crystalline aggregates are shown. Hence, although HA does not exhibit any bioactivity (the in vitro assay of HA was carried out for 8 weeks), the addition of 20% of a bioactive glass causes the growth of the characteristic apatite layer of bioactive material. The kinetics of the formation of the new apatite-like layer, generated from the glass, is favored by the apatite present in the mixture. When in contact with physiological solutions, the process of formation of the new apatite-like layer on the surface of bioactive glass starts with an ionic exchange between the glass and the solution; a pH variation also takes place, and both phenomena lead to the formation of an amorphous calcium phosphate, constituting the nuclei on which the new apatite-like phase grows. When this mechanism starts in the case of BPM, the newly formed phase finds a media with a majority presence of HA (80%). This leads to the formation of calcium phosphate that easily grows onto the surface of the HA component of the BPM, which constitutes an optimum field of nucleation. Glancing-angle XRD allows the HA component of the BPM, much more crystalline, to be distinguished from the newly formed apatite-like layer, with lower crystallinity. The HA component of the BPM acts as a seed for the growth of the new apatite phase. On the other hand, the modification of the HA surface by the growth of the new apatite phase, with low crystallinity and composed by nanometric crystals, facilitates its higher reactivity.

In addition, comparing 55S and BPM bioactivity, the growth of the apatite-like layer seems more homogeneous for the BPM, and this newly formed layer is more crystalline after short times of immersion in SBF. Thus, the higher crystallinity of the BPM layer should be due to the presence of synthetic HA in the material.

Also, EDS patterns are included in Figure 4, in which the following can be observed: the initial composition of the material before soaking in SBF and how after 24 h of soaking in SBF the Si signal from the glass component has disappeared, indicating the formation of the apatite-like layer. The disappearance of the Si signal indicates that the newly formed layer has different chemical composition than the original BPM, in which this signal was present because of the glass component of the mixture. Therefore, the surface of the initial material containing Si seems to be completely covered by a layer composed of calcium phosphates.

In Figure 5 SEM micrographs of the cross section of 55S and BPM after 7 days of soaking in SBF are shown and the thickness of the layer is indicated by a double arrow. In addition, details of both layers are included. As can be observed, although both materials exhibit a newly formed HA layer on its surface, the covering of the BPM surface seems more homogeneous. In addition, the aspect of this layer looks more compact and dense than the one grown on 55S.

The porosity of the three materials was studied by Hg intrusion, following pore evolution during the assay. Figure 6 shows the variation of the intrusion volume as a function of pore diameter for the original glass, BPM, and HA. The bimodal distribution of pores of 55S (macro- and mesopores, with maxima centered at 0.477 and 0.012 μm) can be observed, while HA shows a single

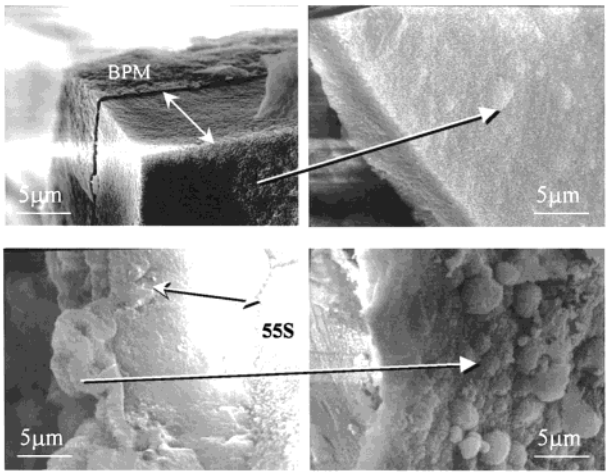

Figure 5. SEM micrographs of the cross section and surface of 55S and BPM are shown after 7 days of immersion in SBF.

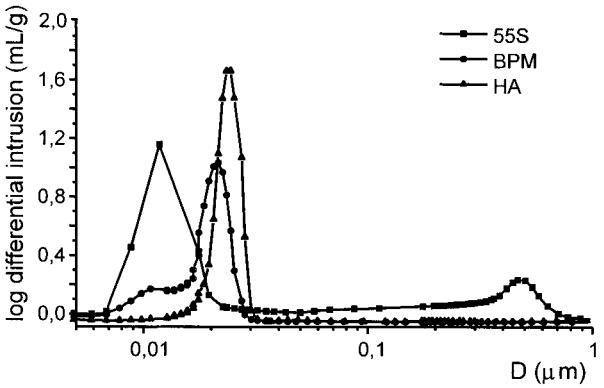

Figure 6. Pore distribution of the starting materials.

maximum, centered at 0.025 μm. The BPM shows an intermediate pore size of 0.022 μm, together with a shoulder centered at 0.011 μm, probably due to the glass component. Besides, the total intrusion volume obtained for 55S, BPM, and HA was 0.59, 0.27, and 0.25 mL/g, respectively. This agrees with the SEM micrographs shown in Figure 4, in which the initial materials presented different aspects, 55S being rather porous and BPM, similar to HA, showing lower porosity. This seems reasonable because the latter do not have macropores. As previously reported,[9] the mesopores' size of 55S does not significantly change during the assay, being almost the same size before and after being soaked for 7 days in SBF. Because no changes in HA porosity are observed, initial and final (after 7 days of immersion in SBF) distribution of pores in the region of 0.005−0.06 μm for both 55S and BPM are shown in Figure 7. For 55S, the porosity of th eoriginal material and the apatite-like phase formed coincide, but the pore size of BPM decreases with time, approaching the 55S final value.

Besides, in the inset of Figure 7 the evolution of the pore diameter (center of pore maximum distribution) with time of soaking in SBF for the BPM is shown. The early increase of pore size of 55S due to the Ca^{2+} release to the media, causing the augmentation of pore diameter, followed by the decrease in size due to the covering of the surface by the apatite-like layer can be observed. However, BPM gradually decreases its pore size from the beginning as long as the apatite-like layer grows.

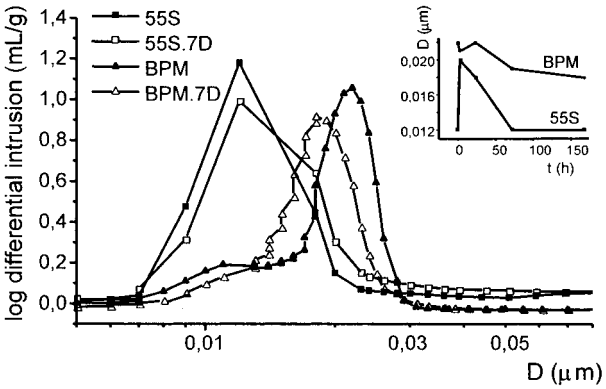

Figure 7. Evolution of pore distribution and pore size as a function of soaking time in SBF for 55S and BPM.

Conclusions

A biphasic material composed of synthetic hydroxyapatite, which emulates the bone mineral component, and a bioactive glass has been synthesized. The potential bioactivity of the starting materials and the mixture has been studied. Although the original hydroxyapatite has not shown any bioactive behavior, the addition of 20 wt % of glass induces the growth of an apatite-like layer on the surface of the biphasic material. The HA component of the BPM acts as a seed for the growth of the new apatite phase, with nanometer size, formed as a consequence of the reactivity of 55S glass.

This new result is very promising in terms of finding a new application of bioactive glasses, whose minority presence in biphasic mixtures with hydroxyapatites of low bioactivity can significantly increase the bioactive response of the implant. That would be a clear example of the symbiosis of two materials, where hydroxyapatite fulfills the composition and structure expectative and the bioactive glass accelerates its bioactivity, achieving a positive response in a short time of 24 h, as opposed to more than 2 months needed for hydroxyapatite itself.

In addition, the newly formed layer is more homogeneous and crystalline than the one formed on the glass itself, which suggests that the hydroxyapatite present in the starting material induces the crystallinity observed in the apatite-like phase formed.

Acknowledgment. Financial support of CICYT, Spain, research project MAT99-0466, is acknowledged.

CM011165P